JHEP PROCEEDINGS

Heavy Flavours 8, Southampton, UK, 1999

Recent Results on Rare b Decays

David E. Jaffe

University of California San Diego

E-mail: djaffe@lns.cornell.edu

ABSTRACT: Recent experimental results on charmless rare b decays are reviewed.

1. Introduction

Recent experimental results on rare b decays are dominated by the CLEO experiment with notable contributions from ALEPH, CDF and D0. I will discuss only results on charmless hadronic B meson decays ($B \to PP, PV$ where $P = \pi$, K, η, η' and $V = \rho$, K^*, ω), radiative b decays and purely leptonic B meson decays . I will omit any discussion of such rare b decays as $B^+ \to D^0 K^+$, $B^+ \to D^{*+} D^{*-}$, $B^+ \to \ell^+ \nu$, and $b \to s\nu\bar{\nu}$.

The search for rare b decays lead to the first observation of penguin decays in exclusive radiative B meson decays [1] and revealed the unexpectedly large role of penguin contributions in charmless hadronic B decays. The interference between the tree and penguin contributions means that B decay rates to charmless hadronic final states are sensitive to γ, the phase of V_{ub} [2]. Several authors have proposed methods to bound γ using ratios of $B \to K\pi$ decay rates [3, 4] with relatively little model dependence. Both methods use $B \to K\pi$ branching fractions to set bounds on γ. Using the preliminary results contained in this paper, neither the Fleischer-Mannel [3] bound

$$\Gamma(B^0 \to K^- \pi^+)/\Gamma(B^+ \to K^0 \pi^+) \geq \sin^2\gamma$$
$$1.11 \pm 0.35 = \sin^2\gamma$$

nor the Neubert-Rosner [4] bound

$$2R_* \equiv \mathcal{B}(B^+ \to K^0\pi^+)/\mathcal{B}(B^+ \to K^+\pi^0)$$
$$(1 - \sqrt{R_*})/\bar{\epsilon}_{3/2} \leq |\delta_{EW} - \cos\gamma|$$
$$0.55 \pm 0.74 \leq |(0.64 \pm 0.15) - \cos\gamma|$$

can set a meaningful limit on γ [5]. Another method seeks to provide information on γ by sacrificing model-independence for comprehensive use of existing measured branching fractions [6].

In addition to probing $\arg(V_{ub}^*)$, the measurement of the proper time dependence of rare B decays to $\pi\pi$ [7] and $\pi\pi\pi$ [8] can yield a measurement of α [2]. Finally, the search for direct CP violation in charmless hadronic and radiative B decays could provide evidence of non-Standard Model (SM) physics.

Table 1 lists the number of b hadrons accumulated by different experiments. The majority of results on charmless hadronic and radiative b decays come from the CLEO experiment that operates just above the $B\bar{B}$ threshold at the $\Upsilon(4S)$ resonance. At $\sqrt{s} \approx 10.6$ GeV, the main source of background is continuum $e^+e^- \to q\bar{q}$ ($q = ucsd$) with a cross-section of ~ 3 nb or about three times $\sigma(B\bar{B})$. A number of features allow the suppression or successful treatment of the continuum by CLEO. Near threshold, the decay products of the $B\bar{B}$ pair are isotropically distributed in contrast to the back-to-back or "jetty" nature of continuum events. CLEO exploits the fact that the B meson energy E_B is the beam energy E_{beam} to form the beam-constrained mass $M_B \equiv \sqrt{{E_{beam}}^2 - \vec{p}_B^{\,2}}$ which is essentially a measure of the momentum balance of the B candidate and has a resolution $\sigma(M_B) \approx 2.5$ MeV dominated by the beam energy spread. CLEO also takes approximately one third of its data about 60 MeV below the $\Upsilon(4S)$ resonance, effectively turning off the production of B mesons and permitting direct evaluation of continuum background processes.

The entire CLEO data sample consists of 9.7×10^6 $B\bar{B}$ pairs with 3.3×10^6 $B\bar{B}$ pairs ac-

Experiment	$\sqrt{s}$ (GeV)	Production rate	Data sample
CLEO	~ 10.6	$\sigma(\mathrm{B\bar{B}}) \sim 1$ nb	$9.7 \times 10^6 \mathrm{B\bar{B}}$
LEP	~ 91	$\sigma(b\bar{b}) \sim 7$ nb	$0.9 \times 10^6 b\bar{b}$/Expt
CDF/D0	1800	$\sigma(b\bar{b}) \sim 100$ μb	trigger dependent

Table 1: Numbers of b hadrons accumlated at different experiments.

cumulated with the CLEO II detector configuration [9]. The remaining 6.4×10^6 $\mathrm{B\bar{B}}$ pairs were accumulated with the CLEO II.V detector configuration [10]. The innermost tracking chamber was replaced by a three-layer, double-sided silicon vertex detector and the argon-ethane gas mixture in the large drift chamber was replaced by helium-propane to convert CLEO II to CLEO II.V. The latter of these detector modifications improves the charged kaon and pion separation both in terms of specific ionization dE/dx measured in the drift chamber and the momentum resolution.

2. Charmless hadronic B decays

Charmless hadronic B decay candidates are selected by requiring $|E_{\mathrm{B}} - E_{\mathrm{beam}}| \equiv |\Delta E| < 200$ or 300 MeV (The ΔE resolution varies from 15 to 25 MeV depending on the final state), $5200 < M_{\mathrm{B}} < 5300$ MeV ($\sigma(M_{\mathrm{B}}) \approx 2.5$ MeV) and $|\cos(\theta_{\mathrm{sphericity}})| < 0.8$ or 0.9 [11]. The $|\Delta E|$ and $|\cos(\theta_{\mathrm{sphericity}})|$ differ slightly for the different decay modes. The latter requirement exploits the difference in the shape of $\mathrm{B\bar{B}}$ and continuum events. In addition loose resonance mass M_{res} and particle identification cuts are used where applicable. Yields are extracted from the sample of resulting B candidates from an unbinned maximum likelihood (ML) fit [12] to the largely independent variables M_{B}, ΔE, $\mathcal{F}$, dE/dx, M_{res} and $\cos\theta_{\mathrm{helicity}}$, where $\mathcal{F}$ is a Fisher discriminant combining 11 event shape variables [12], M_{res} is the $\rho, \mathrm{K}^*, \eta, \eta'$ or ω candidate mass and $\cos\theta_{\mathrm{helicity}}$ is the helicity angle appropriate for pseudoscalar $\to$ pseudoscalar,vector decays. In order to graphically present the results, cuts are applied to all variables in the fit except for the variable being plotted. These cuts generally reduce the signal efficiency by $\sim 50\%$ and the background by an order of magnitude.

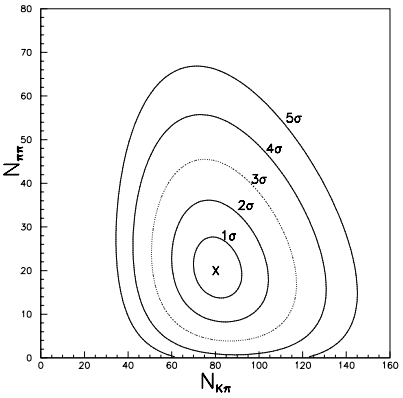

Figure 1: The likelihood contours in intervals of standard deviations (statistical uncertainty only) for the $\mathrm{B}^0 \to \pi^+\pi^-$ *vs.* $\mathrm{B}^0 \to \mathrm{K}^\pm\pi^\mp$ yields.

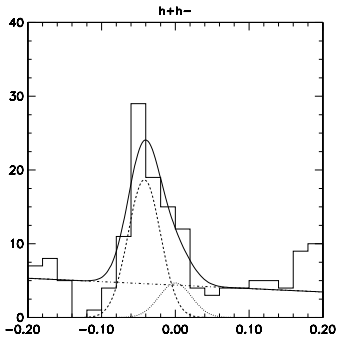

Figure 2: The difference in the $\mathrm{B}^0 \to h^+h^-$ candidate energy and E_{beam} in GeV when both B^0 daughter candidates are assigned the charged pion mass. The solid line represents the full fit, the dashed line represents the $\mathrm{K}^+\pi^-$ component, the dotted line represents the smaller $\pi^+\pi^-$ component, the dot-dash line represents the background and the histogram represents the data.

The preliminary results from the ML fit to $\mathrm{B}^0 \to h^+\pi^-$ candidates in 9.7×10^6 $\mathrm{B\bar{B}}$ pairs are shown in figures 1 and 2. The measured yields for $\mathrm{K}^+\pi^-$ and $\pi^+\pi^-$ are $80.2^{+11.8}_{-11.0}$ and $20.0^{+7.6}_{-6.5}$

events, respectively. This represents the first observation of the decay $B^0 \to \pi^+\pi^-$. Figure 1 shows the likelihood contours in increments of standard deviations (statistical uncertainty only); the $B^0 \to \pi^+\pi^-$ is significant at over four standard deviations. Figure 2 demonstrates one component of CLEO's ability to separate charged kaons and pions; when a kaon is assigned the pion mass, the shift in ΔE is -42 MeV ($\sigma(\Delta E) = 25[20]$ MeV for CLEO II [CLEO II.V]). The K/π separation in dE/dx at $|\vec{p}_h| \approx 2.5$ GeV is $1.7[2.0]\sigma$ in CLEO II [CLEO II.V]. The preliminary results for the branching fractions of $B^0 \to h^+h^-$ decays are $(1.88\,^{+0.28}_{-0.26}\pm0.13)\times10^{-5}$, $(0.47\,^{+0.18}_{-0.15}\pm0.06)\times 10^{-5}$ and $< 0.2\times10^{-5}$ at 90% CL for $h^+h^- = K^+\pi^-$, $\pi^+\pi^-$, and K^+K^-, respectively [13] [1].

The preliminary results for the related decays $B^+ \to K^0h^+$ and $B^+ \to h^+\pi^0$ are $\mathcal{B}(B^+ \to K^0\pi^+) = (1.82^{+0.46}_{-0.40} \pm 0.16)\times10^{-5}$, $\mathcal{B}(B^+ \to K^0K^+) < 0.51\times10^{-5}$ at 90% CL, $\mathcal{B}(B^+ \to K^+\pi^0) = (1.21^{+0.30+0.21}_{-0.28-0.14})\times10^{-5}$ and $\mathcal{B}(B^+ \to \pi^+\pi^0) < 1.2\times10^{-5}$ at 90% CL [13]. Significant signals are seen in decays to $K^0\pi^+$ and $K^+\pi^0$ but not in $\pi^+\pi^0$ or $K^0\pi^+$. The relatively low values of $\mathcal{B}(B^0 \to \pi^+\pi^-)$ and $\mathcal{B}(B^+ \to \pi^+\pi^0)$ with respect to $B^0 \to K^+\pi^-$ and $B^+ \to K^+\pi^0$ indicate that there will be substantial experimental difficulties in addition to the theoretical uncertainties in measuring the angle α of the unitarity triangle (UT) [7].

Figures 3 and 4 shows the beam-constrained mass and $\cos\theta_{\rm helicity}$ distributions for $B^+ \to \rho^0h^+$ candidates in 5.8×10^6 $B\bar{B}$. Both distributions show evidence of a B^+ signal. The yields from the ML fit are $26.1^{+9.1}_{-8.0}$ and $14.8^{+8.8}_{-7.7}$ for $\rho^0\pi^+$ and ρ^0K^+, respectively, corresponding to $\mathcal{B}(B^+ \to \rho^0\pi^+) = (1.5\pm0.5\pm0.4)\times10^{-5}$ and $\mathcal{B}(B^+ \to \rho^0K^+) < 2.2\times10^{-5}$ at 90% CL (preliminary).

For the related decay, $B^0 \to \rho^\pm h^\mp$, only positive values of $\cos\theta_{\rm helicity}$ are considered (Fig. 5). This serves to suppress backgrounds since it selects both a high momentum neutral pion that has less combinatorial background and a low momentum charged pion that is well-separated from $K^\pm$ by dE/dx thus reducing potential backgrounds from $B^0 \to K^{*+}\pi^-$. The preliminary results are

[1] All CLEO results presented here assume $\mathcal{B}(\Upsilon(4S) \to B^0\bar{B}^0) = \mathcal{B}(\Upsilon(4S) \to B^+B^-) = 0.5$

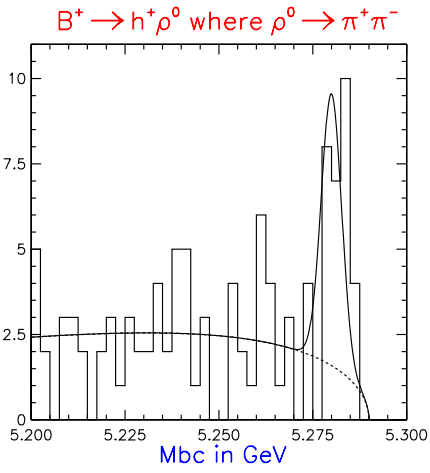

Figure 3: The beam-constrained mass $M_{\rm B}$ distribution for $B^+ \to \rho^0\pi^+$ candidates. The solid line represents the full fit, the dashed line represents the background and the histogram represents the data.

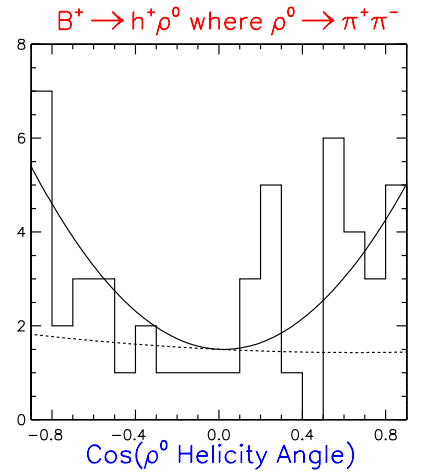

Figure 4: The $\cos\theta_{\rm helicity}$ distribution for $B^+ \to \rho^0\pi^+$ candidates.

$\mathcal{B}(B^0 \to \rho^\pm\pi^\mp) = (3.5\,^{+1.1}_{-1.0} \pm 0.5)\times10^{-5}$ and $\mathcal{B}(B^0 \to \rho^\pm K^\mp) < 2.5\times10^{-5}$ at 90% CL in 7.0×10^6 $B\bar{B}$. In principle, the angle α could be measured to a precision of $\sim 6^\circ$ with a likelihood fit to the proper time-dependence of the $\pi^+\pi^-\pi^0$ Dalitz distribution with ~ 1000 *background-free* $B^0 \to \pi^+\pi^-\pi^0$ events [8]. Given CLEO's result, such a measurement would require over 100 fb^{-1} at an asymmetric, e^+e^- B-factory and would be complicated by the backgrounds as shown in figure 6. In addition, the region of the Dalitz distri-

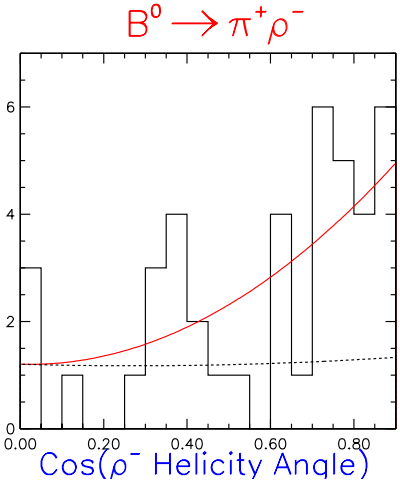

Figure 5: The $\cos\theta_{\rm helicity}$ distribution for $B^0 \to \rho^\pm\pi^\mp$ candidates.

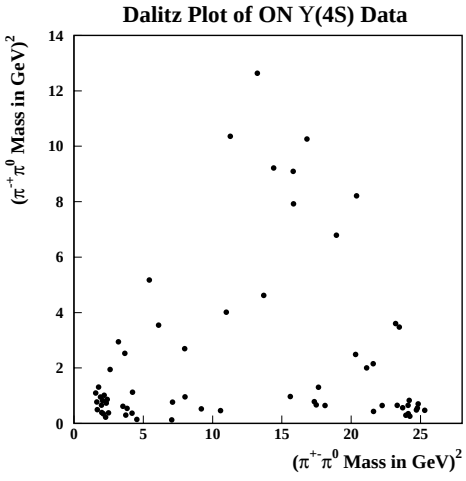

Figure 6: The Dalitz distribution ($M^2(\pi^\pm\pi^0)$ *vs.* $M^2(\pi^\mp\pi^0)$) for $B^0 \to \pi^+\pi^-\pi^0$ candidates. To improve the visibility of the ρ resonance, the plot is "folded": the larger (smaller) of $M^2(\pi\pi^0)$ is plotted on the horizontal (vertical) axis.

bution most sensitive to α due to the interference between $B^0 \to \rho^+\pi^-$ and $B^0 \to \rho^-\pi^+$ occurs when $M^2(\pi^+\pi^0) \sim M^2(\pi^-\pi^0) \sim M^2(\rho)$ where the backgrounds to neutral pions are largest.

The likelihood contours for $B^+ \to \omega h^+$ are shown in Figure 7 for 9.7×10^6 $B\bar{B}$. The yield of $B^+ \to \omega\pi^+$ (ωK^+) is determined to be $28.5^{+8.2}_{-7.3}$ ($7.9^{+6.0}_{-4.7}$) corresponding to $\mathcal{B}(B^+ \to \omega\pi^+) = (1.1 \pm 0.3 \pm 0.1) \times 10^{-5}$ and $\mathcal{B}(B^+ \to \omega K^+) < 0.8 \times 10^{-5}$ at 90% CL [14]. The $B^+ \to \omega\pi^+$ branching fraction is consistent with that of $B^+ \to \rho^0\pi^+$ as expected from isospin. The limit on the $B^+ \to \omega K^+$ branching fraction is somewhat at odds with CLEO's earlier reported value of $(1.5^{+0.7}_{-0.6} \pm 0.2) \times 10^{-5}$ in the 3.3×10^6 $B\bar{B}$ of the CLEO II data sample [15]. Two factors are responsible for this change. The CLEO II data sample was re-analyzed with improved calibration and track-fitting allowing an extension of the geometric acceptance and track quality requirements resulting in an increase in reconstruction efficiency of 10 to 20%. The re-analysis reduced the ωK^+ yield and increased the $\omega\pi^+$ yield. In addition, there were very few ωK^+ candidates found in the CLEO II.V data sample (6.4×10^6 $B\bar{B}$).

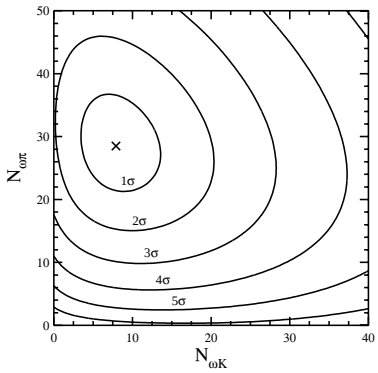

Figure 7: The likelihood contours for the $B^+ \to \omega\pi^+$ *vs.* $B^+ \to \omega K^+$ yields.

The beam-constrained mass distributions for $B^+ \to \eta' K^+$ and $B^0 \to \eta' K^0$ are shown in figures 8 and 9. The corresponding, preliminary branching fractions from 9.7×10^6 $B\bar{B}$ are $\mathcal{B}(B^+ \to \eta' K^+) = (8.0^{+1.0}_{-0.9} \pm 0.8) \times 10^{-5}$, $\mathcal{B}(B^0 \to \eta' K^0) = (8.8^{+1.8}_{-1.6} \pm 0.9) \times 10^{-5}$ and $\mathcal{B}(B^+ \to \eta'\pi^+) < 1.1 \times 10^{-5}$ at 90% CL [16]. These surprisingly large branching fractions are compared to predictions in table 2. Disparate explanations of the large $B \to \eta' K$ branching fractions have been offered such as a large gluonic [18] or intrinsic charm [19] content of the η'. Lipkin extended isospin and flavor symmetry treatment of B decays to include final state interactions and proposed the sum rule [20]

$$\mathcal{B}(B^+ \to \eta' K^+) + \mathcal{B}(B^+ \to \eta K^+) = \mathcal{B}(B^+ \to K^+\pi^0) + \mathcal{B}(B^+ \to K^0\pi^+)$$

which can be evaluated with CLEO measurements

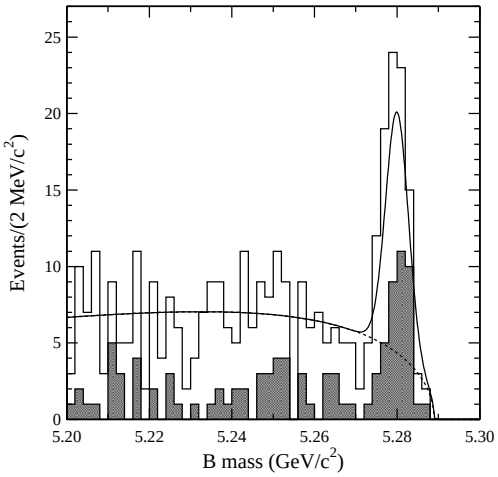

Figure 8: The beam-constrained mass for $B^+ \to \eta' K^+$ candidates. The shaded (white) region represents η' candidates reconstructed in the $\eta' \to \pi^+\pi^-\eta$ ($\rho\gamma$) decay modes.

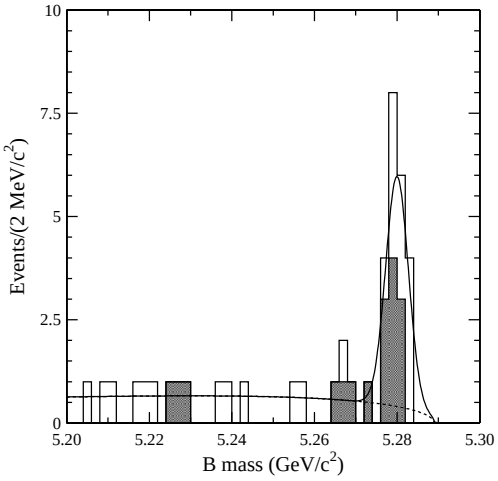

Figure 9: The beam-constrained mass for $B^0 \to \eta' K^0_s$ candidates. The shaded (white) region represents η' candidates reconstructed in the $\eta' \to \pi^+\pi^-\eta$ ($\rho\gamma$) decay modes.

and limits at 90% CL listed in tables 2 and 3 (units are 10^{-5})

$$(8.0^{+1.0}_{-0.9} \pm 0.8) \; + \; (< 0.71) \stackrel{?}{=}$$
$$(1.21^{+0.30+0.21}_{-0.28-0.14}) \; + \; (1.82^{+0.46}_{-0.40} \pm 0.16) \quad .$$

The equality is violated by more than three standard deviations. Recent work [21] suggests that the large $\eta' K$ and ηK^* rates with respect to $\eta' K^*$ and ηK are due to constructive interference of two comparable penguin amplitudes rather than mechanisms specific to the η'.

The summary of CLEO's charmless hadronic B decay measurements is shown in table 3. There is now clear evidence of hadronic $b \to u$ transitions ($B^0 \to \pi^+\pi^-$, $B \to \rho/\omega\pi$). The pattern of $\mathcal{B}(B \to K\pi) \approx \mathcal{B}(B \to \rho/\omega\pi) > \mathcal{B}(B \to \pi\pi)$ is an indication of the constructive [destructive] interference between tree and penguin contributions for $B^0 \to K^+\pi^-$ and $B \to \rho/\omega\pi$ [$B^0 \to \pi^+\pi^-$].

3. Radiative and leptonic b decays

Both ALEPH [23] and CLEO [24] employ similar techniques to measure the $b \to s\gamma$ branching fraction. Photons from π^0s and ηs are vetoed in the selection of the high energy photon candidate. ALEPH suppresses the light quark (*ucsd*) background by imposing a lifetime-based b-tag in the hemisphere opposite the photon candidate. At CLEO, the suppression of the *ucsd* background is achieved by a neural network that utilizes event shape information. Both experiments then form an X_s candidate from a combination of tracks, K^0_s and π^0 candidates that, when combined with the high energy photon, produces the "best" b hadron candidate. The photon energy spectra from the remaining candiates are shown in figures 10 and 11. The subtraction of the remaining background is accomplished quite differently by the two experiments. CLEO takes advantage of the data accumulated below the $B\bar{B}$ threshold to subtract the dominant *ucsd* background. ALEPH adjusts their simulation of the background processes based on $b \to s\gamma$-poor regions of distributions that discriminate between signal and background. This procedure reduces ALEPH's sensitivity to their simulation but increases the systematic uncertainty. The measured $b \to s\gamma$ branching fractions of $(3.15 \pm 0.35 \pm 0.32 \pm 0.26) \times 10^{-4}$ and $(3.11 \pm 0.80 \pm 0.72) \times 10^{-4}$ from CLEO and ALEPH, respectively, are in good agreement with the SM calculation at next-to-leading order of $(3.28 \pm 0.33) \times 10^{-4}$ [25]. The CLEO result is preliminary and based on 3.3×10^6 $B\bar{B}$.

Even though the $b \to s\gamma$ rate agrees with the SM calculation, many non-SM effects could give rise to a sizeable ($\sim$ 40%) rate asymme-

Reaction	$\mathcal{B}$ or UL ($\times 10^{-5}$)	Prediction	$N(\mathrm{B\bar{B}})(\times 10^6)$	Reference
$\mathrm{B}^+ \to \eta' \mathrm{K}^+$	$8.0^{+1.0}_{-0.9} \pm 0.8$	2.1-4.1	9.7	[16]
$\mathrm{B}^0 \to \eta' \mathrm{K}^0$	$8.8^{+1.8}_{-1.6} \pm 0.9$	2.1-4.1	9.7	[16]
$\mathrm{B}^+ \to \eta' \mathrm{K}^{*+}$	< 8.7	0.03-0.04	6.7	[17]
$\mathrm{B}^0 \to \eta' \mathrm{K}^{*0}$	< 2.0	0.01-0.04	6.7	[17]
$\mathrm{B}^+ \to \eta \mathrm{K}^+$	< 0.71	0.2-0.4	9.7	[16]
$\mathrm{B}^0 \to \eta \mathrm{K}^0$	< 0.95	0.2-0.4	9.7	[16]
$\mathrm{B}^+ \to \eta \mathrm{K}^{*+}$	$2.73^{+0.96}_{-0.82} \pm 0.50$	0.2-0.3	9.7	[16]
$\mathrm{B}^0 \to \eta \mathrm{K}^{*0}$	$1.38^{+0.55}_{-0.44} \pm 0.17$	0.2-0.3	9.7	[16]

Table 2: Preliminary CLEO results for $B \to \eta(')\mathrm{K}^*$ compared to predictions from Ref. [22].

Decay	$\mathcal{B}$ or UL ($\times 10^{-5}$)	Decay	$\mathcal{B}$ or UL ($\times 10^{-5}$)
$\mathrm{B}^0 \to \mathrm{K}^+\pi^-$	$1.88\ ^{+0.28}_{-0.26} \pm 0.13$	$\mathrm{B}^0 \to \mathrm{K}^{*\pm}\pi^\mp$	$2.2\ ^{+0.8}_{-0.6}\ ^{+0.4}_{-0.5}$
		$\mathrm{B}^0 \to \rho^\pm \mathrm{K}^\mp$	< 2.5
$\mathrm{B}^+ \to \mathrm{K}^+\pi^0$	$1.21^{+0.30+0.21}_{-0.28-0.14}$	$\mathrm{B}^+ \to \rho^0 \mathrm{K}^+$	< 2.2
		$\mathrm{B}^+ \to \omega \mathrm{K}^+$	< 0.8
$\mathrm{B}^+ \to \mathrm{K}^0\pi^+$	$1.82^{+0.46}_{-0.40} \pm 0.16$		
$\mathrm{B}^0 \to \pi^+\pi^-$	$0.47\ ^{+0.18}_{-0.15} \pm 0.06$	$\mathrm{B}^0 \to \rho^\pm\pi^\mp$	$3.5\ ^{+1.1}_{-1.0} \pm 0.5$
$\mathrm{B}^+ \to \pi^+\pi^0$	< 1.2	$\mathrm{B}^+ \to \rho^0\pi^+$	$1.5 \pm 0.5 \pm 0.4$
		$\mathrm{B}^+ \to \omega\pi^+$	$1.1 \pm 0.3 \pm 0.1$
$\mathrm{B}^0 \to \mathrm{K}^+\mathrm{K}^-$	< 0.2	$\mathrm{B}^0 \to \mathrm{K}^{*\pm}\mathrm{K}^\mp$	< 0.6
$\mathrm{B}^+ \to \mathrm{K}^0\mathrm{K}^+$	< 0.51		

Table 3: Summary of charmless hadronic branching fractions ($\mathcal{B}$) or upper limits (UL) at 90% CL.

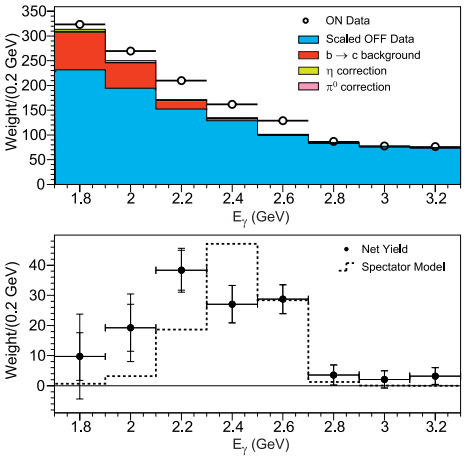

Figure 10: The photon energy spectrum for $b \to s\gamma$ candidates from the CLEO experiment. The upper (lower) figure shows the distribution before (after) background subtraction.

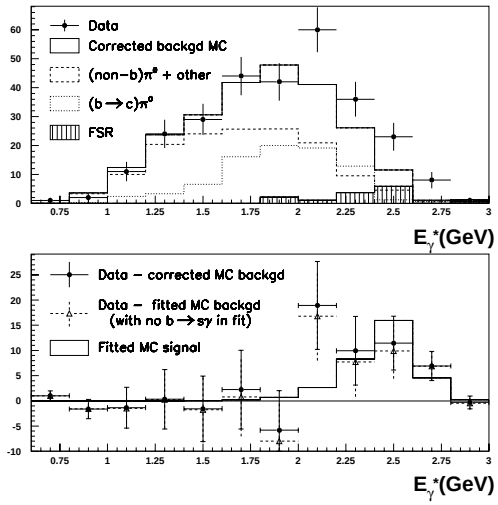

Figure 11: The photon energy spectrum for $b \to s\gamma$ candidates from the ALEPH experiment. The upper (lower) figure shows the distribution before (after) background subtraction.

try [26]. CLEO extends their X_s reconstruction method to "tag" the b-flavor of the final state of the $b \to s\gamma$ decay to produce a measurement of the asymmetry

$$\mathcal{A}^0 \equiv \frac{\Gamma(b \to s\gamma) - \Gamma(\bar{b} \to \bar{s}\gamma)}{\Gamma(b \to s\gamma) + \Gamma(\bar{b} \to \bar{s}\gamma)} \quad . \qquad (3.1)$$

Monte Carlo is used to determine the rate of the three possible outcomes of tagging: 1) b flavor determinable and correctly assigned, 2) b flavor determinable and incorrectly assigned or 3) b flavor not determinable. The preliminary CLEO result, based on 3.3×10^6 $B\bar{B}$, for the measured asymmetry, after both additive and multiplicative corrections, is $\mathcal{A}^0 \approx \mathcal{A}^{\rm meas} = (0.16 \pm 0.14_{\rm stat} \pm 0.05_{\rm syst}) \times (1.000 \pm 0.041)_{\rm syst}$ or $-0.09 < \mathcal{A}^{\rm meas} < 0.42$ at 90% CL.

Hadron collider experiments are currently only sensitive to rare b decays containing charged lepton pairs due to their triggering ability. CDF exploits this sensitivity to search for the decays $B \to K^{(*)}\mu^+\mu^-$ [27]. The candidates for these decays must form a common vertex (χ^2(vertex) $<$ 20) with a measured decay length greater than 400 microns transverse to the $p\bar{p}$ collision axis. In addition the $B \to K^{(*)}\mu^+\mu^-$ candidates must satisfy an isolation requirement that takes advantage of the hard fragmentation of b quarks. Figures 12 and 13 show the $M(\mu^+\mu^-)$ *vs.* $M(K^{(*)}\mu^+\mu^-)$ distributions for the $B^+ \to K^+\mu^+\mu^-$ and $B^0 \to K^{*0}\mu^+\mu^-$ candidates. The candidates due to $B \to \psi^{(\prime)}K^{(*)}$ decays dominate the distributions which are otherwise relatively background free. The limits obtained by CDF [27] in table 4 are within an order of magnitude of the SM prediction and indicate that this decay should be observed with the increase in luminosity (~ 2 fb^{-1}) expected for the upcoming run. The measurement of the dilepton mass spectrum and the lepton-pair forward-backward asymmetry are important for the separation of the long- and short-distance contributions to the decay [28] and are sensitive to contributions from non-SM processes [29], but will require another order of magnitude increase in luminosity.

Table 4 also lists results of searches for the inclusive decay $b \to s\ell^+\ell^-$ by D0 [30] and CLEO [31]. CLEO adapts their inclusive X_s reconstruction from the $b \to s\gamma$ measurement while D0 simply searches for high-mass lepton pairs below the B mass and above the charmonium resonances. All measurements are at least an order of magnitude higher than SM expectations.

Both CDF and CLEO have searched for the purely leptonic b decays $B^0 \to \ell^+\ell^-$ as listed in table 5. The current upper limits are at least several orders of magnitude above the SM expectations. The SM $B_s^0 \to \mu^+\mu^-$ decay rate should observable with the full expected luminosity from CDF's upcoming run if backgrounds can be reduced and the overall detection efficiency enhanced by at least a factor of two.

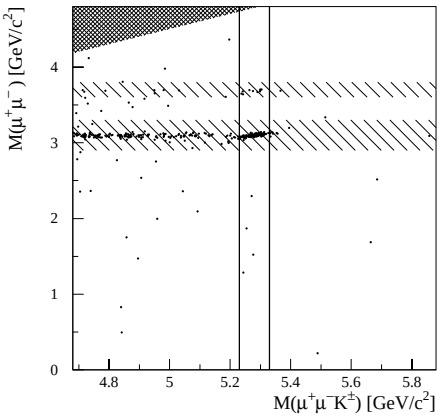

Figure 12: The $M(\mu^+\mu^-)$ *vs.* $M(K^+\mu^+\mu^-)$ distribution for $B^+ \to K^+\mu^+\mu^-$ candidates from CDF. The vertical lines delineate the signal region, the diagonal hatching shows the excluded ψ and ψ' regions and the shaded region is kinematically forbidden.

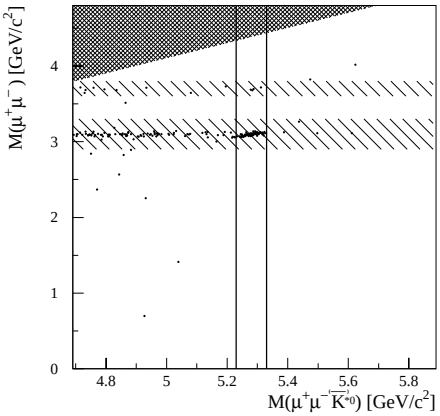

Figure 13: The $M(\mu^+\mu^-)$ *vs.* $M(K^{*0}\mu^+\mu^-)$ distribution for $B^0 \to K^{*0}\mu^+\mu^-$ candidates from CDF.

Expt	$\mathcal{B}(\mathrm{B}^+ \to \mathrm{K}^+\ell^+\ell^-)$	$\mathcal{B}(\mathrm{B}^0 \to \mathrm{K}^{*0}\ell^+\ell^-)$	$\mathcal{B}(b \to s\ell^+\ell^-)$
CDF ($\ell = \mu$)	$< 5.2 \times 10^{-6}$	$< 4.0 \times 10^{-6}$	
D0($\ell = \mu$)			$< 3.2 \times 10^{-4}$
CLEO($\ell = \mu$)	$< 9.7 \times 10^{-6}$	$< 9.5 \times 10^{-6}$	$< 5.7 \times 10^{-5}$
CLEO($\ell = e$)	$< 11 \times 10^{-6}$	$< 13 \times 10^{-6}$	$< 5.8 \times 10^{-5}$
CLEO(μ & e)			$< 4.2 \times 10^{-5}$
Std Model	$(0.3 - 0.7) \times 10^{-6}$	$(1 - 4) \times 10^{-6}$	$\sim 6 \times 10^{-6}$
CLEO $\mu^\pm e^\mp$			$< 2.2 \times 10^{-5}$

Table 4: Summary of $\mathrm{B} \to \mathrm{K}^{(*)}\ell^+\ell^-$ and $b \to s\ell\ell$ searches. All upper limits are at 90% CL.

Decay	CDF Upper limit at 95% CL	CLEO Upper limit at 90% CL	SM expectation
$\mathrm{B}^0_\mathrm{d} \to \mu^+\mu^-$	$< 8.6 \times 10^{-7}$	$< 5.9 \times 10^{-6}$	2×10^{-10}
$\mathrm{B}^0_\mathrm{d} \to e^+e^-$		$< 5.9 \times 10^{-6}$	3×10^{-15}
$\mathrm{B}^0_\mathrm{s} \to \mu^+\mu^-$	$< 2.6 \times 10^{-6}$		4×10^{-9}
$\mathrm{B}^0_\mathrm{d} \to e^\pm\mu^\mp$	$< 8.2 \times 10^{-6}$	$< 5.9 \times 10^{-6}$	0
$\mathrm{B}^0_\mathrm{s} \to e^\pm\mu^\mp$	$< 4.5 \times 10^{-6}$		0

Table 5: Summary of $\mathrm{B}^0 \to \ell^+\ell^-$ searches.

4. Conclusions

As the era of the b factories begins, the current knowledge of charmless hadronic b decays indicates that independent measurement of the angles α and γ of the unitarity triangle will be difficult. The relatively low rate of $\mathrm{B}^0 \to \pi^+\pi^-$ with respect to $\mathrm{B}^0 \to \mathrm{K}^+\pi^-$ will hamper efforts to measure the time-dependent CP asymmetry of $\mathrm{B}^0 \to \pi^+\pi^-$. The apparently large penguin contributions to $\mathrm{B} \to \pi\pi$ will also complicate the extraction of α from the measured asymmetry. An alternative proposal to measure α with $\mathrm{B} \to \pi\pi\pi$ decays will require years of running at the asymmetric, $\mathrm{e^+e^-}$ B-factories and may only be feasible at $p\bar{p}$ colliders. The complications to the measurement of α due to large penguin-tree interference may make it possible to measure or bound the angle γ; however, current measurements and methods are unable to provide meaningful bounds or are model dependent. While $\sin 2\beta$ will almost surely be measured with significant precision and reported at the 9$^{\mathrm{th}}$ International Symposium on Heavy Flavor Physics, measurements of α and γ of comparable precision from rare b decays may well have to wait for future conferences.

References

[1] R. Ammar *et al.*, *Phys. Rev. Lett.* **71** (1993) 674.

[2] C. Caso *et al.*, *Eur. Phys. J.* **C 3** (1998) 1.

[3] R. Fleischer and T. Mannel, *Phys. Rev.* **D 57** (1998) 2752.

[4] M. Neubert and J. Rosner, *Phys. Lett.* **B 441** (1998) 403; M. Neubert, *J. High Energy Phys.* **9902** (1999) 014

[5] The overall uncertainty in the Kπ branching fractions used to compute R and R_* is estimated as the sum in quadrature of the larger of the reported asymmetric statistical and systematic uncertainties. Any correlations between the systematic uncertainties are ignored in forming the ratios. For the Fleischer-Mannel [3] bound: $\tau(\mathrm{B}^+)/\tau(\mathrm{B}^0) = 1.07 \pm 0.02$ determined by the LEP B lifetime working group for Summer 1999, and for the Neubert-Rosner [4] bound: $\delta_{\mathrm{EW}} = 0.64 \pm 0.15$, $\bar{\epsilon}_{3/2} = 0.64 \pm 0.15$.

[6] W.-S. Hou, J. G. Smith and F. Würthwein, `hep-ph/9910014`.

[7] M. Gronau and D. London, *Phys. Rev. Lett.* **65** (1990) 3381; M. Gronau *et al.*, *Phys. Rev.* **D 52** (1995) 6374.

[8] A. Snyder and H. Quinn, *Phys. Rev.* **D 48** (1993) 2139.

[9] Y. Kubota *et al.*, *Nucl. Inst. Meth.* **A 320** (1992) 66.

[10] T. S. Hill, *Nucl. Inst. Meth.* **A 418** (1998) 32.

[11] J. D. Bjorken and S. J. Brodsky, *Phys. Rev.* **D 1** (1970) 1416.

[12] D. M. Asner *et al.*, *Phys. Rev.* **D 53** (1996) 1039 contains a description of the unbinned ML fitting method and the Fisher variable $\mathcal{F}$.

[13] Y. Kwon *et al.*, `hep-ex/9908039`.

[14] M. Bishai *et al.*, `hep-ex/9908018`.

[15] T. Bergfeld *et al.*, *Phys. Rev. Lett.* **81** (1998) 272.

[16] S. J. Richichi *et al.*, `hep-ex/9908019`.

[17] Y.Gao and F.Würthwein, `hep-ex/9904008v2`.

[18] M. R. Ahmood, E. Kou and A. Sugamoto,*Phys. Rev.* **D 58** (1998) 014015; D. S. Du, C. S. Kim and Y. D. Yang, *Phys. Lett.* **B 419** (1998) 369; D. S. Du, Y. D. Yang and G. Zhu, *Phys. Rev.* **D 59** (1999) 014007; D. S. Du, Y. D. Yang and G. Zhu, *Phys. Rev.* **D 60** (1999) 054015.

[19] I. Halperin and A. Zhitnitsky, *Phys. Rev.* **D 56** (1998) 7247; E. V. Shuryak and A. Zhitnitsky, *Phys. Rev.* **D 57** (1998) 2001.

[20] H. J. Lipkin, *Phys. Lett.* **B 433** (1998) 117.

[21] H.-Y. Chang and K.-C. Yang, `hep-ph/9910291`.

[22] Ali, Kramer and Lü, *Phys. Rev.* **D 58** (1998) 094009.

[23] R. Barate *et al.*, *Phys. Lett.* **B 429** (1998) 169.

[24] S. Ahmed *et al.*, `hep-ex/9908022v2`.

[25] K. Chetykin *et al.*, *Phys. Lett.* **B 400** (1997) 206; A. Kagan and M. Neubert, *Eur. Phys. J.* **C 7** (1999) 5.

[26] A. Kagan and M. Neubert, *Phys. Rev.* **D 58** (1998) 094012; M. Aoki, G. Cho and N. Oshimo, *Phys. Rev.* **D 60** (1999) 035004.

[27] T.Affolder *et al.*, `hep-ex/9905004`, to be published in Physical Review Letters.

[28] N. G. Deshpande, J. Trampetic and K. Panrose, *Phys. Rev.* **D 39** (1989) 1461.

[29] A. Ali, T. Mannel and T. Morozumi, *Phys. Lett.* **B 273** (1991) 505; A. Ali, G. F. Guidice and T. Mannel, *Z. Physik* **C 67** (1995) 471; C. Greub, A. Ioannissian and D. Wyler, *Phys. Lett.* **B 346** (1995) 149; G. Burdman, *Phys. Rev.* **D 52** (1995) 6353.

[30] B. Abbott *et al.*, *Phys. Lett.* **B 423** (1998) 419.

[31] S. Glenn *et al.*, *Phys. Rev. Lett.* **80** (1998) 2289.